Micro-Raman mapping of the polymorphs of serpentine

Journal of RAMAN SPECTROSCOPY

Micro-Raman mapping of the polymorphs of serpentine.

Journal:	*Journal of Raman Spectroscopy*
Manuscript ID:	JRS-14-0297.R2
Wiley - Manuscript type:	Research Article
Date Submitted by the Author:	n/a
Complete List of Authors:	Petriglieri, Jasmine Rita; University of Parma, Department of Physics and Earth Sciences Salvioli-Mariani, Emma; University of Parma, Department of Physics and Earth Sciences Mantovani, Luciana; University of Parma, Department of Physics and Earth Sciences Tribaudino, Mario; University of Parma, Department of Physics and Earth Sciences Lottici, Pier Paolo; University of Parma, Department of Physics and Earth Sciences Laporte-Magoni, Christine; University of New Caledonia, Laboratoire de Geosciences et Physique de la Matiere Condensee LGPMC Bersani, Danilo; University of Parma, Department of Physics and Earth Sciences
Keywords:	Serpentine minerals, Koniambo massif, OH bands, Raman micro-mapping, asbestos

Micro-Raman mapping of the polymorphs of serpentine.

J. R. Petriglieri, [a,b] E. Salvioli-Mariani, [a] L. Mantovani, [a] M. Tribaudino, [a] P. P. Lottici, [a] C. Laporte-Magoni, [b] and D. Bersani, [a]

[a] Department of Physics and Earth Sciences, University of Parma, Parco Area delle Scienze 7/A, 43124 Parma, Italy
[b] Laboratoire PPME, Université de la Nouvelle Calédonie, Campus de Nouville, BP R4 - 98851 Nouméa CEDEX, Nouvelle Caledonie.

Abstract
Serpentinites are rocks, often used in buildings, formed in large extent by minerals of the serpentine group: chrysotile, antigorite, lizardite and polygonal serpentine. The fibrous type (e.g. chrysotile) of serpentine group minerals, along with several amphibole varieties (e.g. actinolite, tremolite), are the major components of asbestos family. The exposure to fine fibrous asbestos powder is linked to diseases such as pleural mesothelioma and asbestosis. The identification of the main varieties of the serpentine group, laminated or fibrous, becomes an issue of great interest for public health. This work introduces an analytical strategy able to distinguish the different serpentine polymorphs directly on the sample, allowing the analysis within their textural environment, evidencing at the micrometer scale the mineral reactions of the phases. Samples coming from the Koniambo massif (Grande Terre island, New Caledonia) were studied by means of optical microscopy, SEM-EDS and Raman spectroscopy. Raman peaks observed in the high-wavenumbers spectral range 3550-3850 cm^{-1}, associated with OH stretching vibrations, allow the discrimination of the all four serpentine varieties. The relationship between the different varieties of serpentine, at a micrometric scale, in complex samples, has been investigated by two-dimensional Raman mapping.

Keywords: Serpentine minerals; Koniambo massif; OH bands; Raman micro-mapping, asbestos.

Introduction

Serpentinites are hydrated mafic and ultramafic rocks constituted mostly by serpentine group minerals: chrysotile, antigorite, lizardite and polygonal serpentine. Belonging to the group of the green stones, serpentinites have long been used by many cultures around the world - Mediterranean, Asia-Oceania, Americas areas - as building and carving stones.
The serpentine group is composed by hydrous minerals (about 13 wt% H_2O) formed during the relative low-temperature hydration of peridotites, dunites and piroxenites, by the alteration of Mg-rich olivine and orthopyroxene [1,2]. Serpentinites play an essential role in numerous geological settings and control the rheology of the lithosphere where aqueous fluids interact with ultramafic rocks [2].
The Mg-rich serpentine minerals are trioctahedral phyllosilicates type 1:1; they present a structural complexity due to the lattice mismatch between the octahedral (O) and the tetrahedral (T) layers. The compensation of the mismatch occurs by chemistry changes or through a curvature of the layers. The microstructure of the four main varieties is based on the change of curvature of the tetrahedral-octahedral layer structure [3,4]. Lizardite has a flat crystal structure, where the planar sheet presents an ideal layer topology. Antigorite shows a corrugated-wavy layer characterized by a modulated structure. Chrysotile with the cylindrical-spiral wrapping of the 1:1 layers exhibits a fibrous structure [5], and polygonal serpentine alternating the presence of flat and curved sectors displays an intermediate structure between chrysotile and lizardite varieties [6,7]. The four varieties of serpentine are not polymorphs *stricto sensu*. In fact, the general formula adopted for chrysotile is $Mg_3Si_2O_5(OH)_4$, while antigorite presents a small $Mg(OH)_2$ depletion due to the inversions in

curvature. In lizardite some different cations are required to stabilize the structure and its formula should be written as $(Mg_{3-x}M_x)$ $[Si_{2-x}M_xO_5(OH)_4]$ where M = Al, Fe, Cr and x is usually around 0.1 [6]. Hydroxyls are present in all serpentine minerals in two different positions: at the center of the six-fold ring of SiO_4 tetrahedra in the T layer (inner OH groups) and in the interlayer space linked to the O layer (outer OH groups)[8]. Due to their coiled habit, chrysotile and polygonal serpentine are the predominant fibrous forms of serpentine group. These minerals, along with several amphibole varieties (e.g. actinolite, tremolite), are the main components of the asbestos family. Inhalation of fine fibrous asbestos powder is known to be a serious health hazard [9–12]. Toxicity of antigorite is still debated, being considered as an asbestos only in some countries. The identification of the laminated or fibrous polymorphs of the serpentine group in petrological samples (rocks, soils, carving stones), building materials and biological tissues (e.g. lung tissue) becomes of great importance for public health problems and for the safety of the operators.

Recent experimental studies, based on vibrational spectroscopies, allowed to clearly recognize the vibrational bands of OH groups of the water molecules for the four polymorphs [8,13–17]. Raman spectroscopy has proven to be the most decisive technique during the discrimination of the varieties: Raman peaks observed in the high-wavenumbers spectral range (3550 - 3850 cm^{-1}) corresponding to the OH stretching vibrations, allowed the identification of the serpentine minerals [8,17].

Despite the recent developments, a methodology able to distinguish the asbestos minerals directly on the sample, without removing the fibers from the rock matrix, has not yet been presented. This work aims at introducing an analytical strategy, based on micro-Raman spectroscopy, able to recognize the four main serpentine polymorphs at the micrometer scale. In particular, Raman micro-mapping in the OH-stretching spectral region, is used to study the presence and the microscopic structural and textural relationships of the different serpentine polymorphs, for a deeper understanding of the serpentinization process.

Experimental

A series of thin sections, obtained from ten rock fragments collected in the Koniambo Massif (Grande Terre Island, New Caledonia), was analyzed in this work. Samples consist in strongly serpentinized harzburgite-dunite and spinel-dunite. Sampling and macroscopic identification were performed by the Laboratoire PPME of the Université de la Nouvelle Calédonie. Optical microscopy, polarizing microscopy, scanning electron microscopy with energy-dispersive X-ray spectrometry (SEM-EDXS) and Raman spectroscopy analysis were performed at the Department of Physics and Earth Sciences of the University of Parma.

Morphological and chemical analyses were carried out with a Jeol 6400 scanning electron microscope equipped with an Oxford EDXS. Operating conditions were 15 kV and 1.2 nA, electron beam of about 1 mm in diameter and 60s counting time; errors are ±2-5% for major elements and ±5-10% for minor components. Standards comprise pure elements, simple oxides or simple silicate compositions.

Non-polarized micro-Raman spectra have been obtained on thin sections in nearly backscattering geometry with a Horiba Jobin-Yvon LabRam apparatus, equipped with an Olympus microscope with 10×, 50×, ULWD 50× and 100× objectives and a motorized x–y stage. The 632.8-nm line of a He–Ne laser and the 473.1-nm line of a doubled Nd:YAG diode pumped laser have been used as excitation; laser power has been controlled by means of a series of density filters, in order to avoid heating effects. The minimum lateral resolution was about 1 μm (with the 100× objective), the depth resolution was set to few micrometers by means of a confocal hole. The spectral resolution is about 2 and 4 cm^{-1} at the 632.8 and 473.1 nm excitation wavelength, respectively. The system was calibrated using the 520.6 cm^{-1} Raman peak of silicon before each experimental session. In addition, in the high wavenumber range, the spectra were constantly calibrated using spectral lamps. The 632.8-nm line was mostly used to obtain high resolution spectra in the low wavenumber range (100-1200 cm^{-1}), whereas the 473.1-nm source was utilized to enhance the OH stretching signal of

the water molecules in the high wavenumber range (3000-4000 cm^{-1}). The spectra were collected using the 100x objective with repeated acquisition: 5 acquisition for 60 s and 25 for 3 s in the low and high-wavenumbers spectral range, respectively. The background subtraction on each spectrum was performed with LabSpec® software.

Raman maps were obtained on a square or rectangular matrix of points: typical size was 25x25 points, with a step between 1 and 2 micrometers. The acquisition time for each point was about 60 s. The false color images were obtained by associating the intensities of the different colors to the area of the OH stretching bands characteristic of the different polymorphs. The areas were determined by fitting of the Raman spectra using gauss-lorentzian functions, after a proper background removal. Some smoothing in the digital maps were performed to overlap them to the photographs of the corresponding analyzed areas.

Results and discussion

Raman spectra of the serpentine polymorphs

Before starting with the detailed analysis of the thin sections, we collected on the Koniambo samples point Raman spectra of the different serpentine polymorphs. The identification of the polymorphs was made by comparison, both in low- and high-wavenumbers regions, with literature [8,15–17] and with spectra on reference materials present in the Department of Physics and Earth Science of the University of Parma.

Raman spectra of serpentine polymorphs in the low-wavenumbers spectral range (150-1100 cm^{-1}), corresponding to the inner vibrational modes of the lattice and to Si-O_4 vibrations, appear quite comparable (Fig. 1). Polygonal serpentine is not present in figure 1 because we were not able to obtain a clear identification of this phase based on the low-wavenumber part on the Raman spectrum. On the other hand, Raman peaks in the 3550-3850 cm^{-1} range, associated with the stretching vibrations of OH groups of the water molecules, allow the identification of all the four polymorphs (Fig. 2).

Table 1 shows the wavenumbers of the characteristic vibrational modes and of the OH stretching vibrations for the main serpentine polymorphs.

Low-wavenumbers Raman spectra obtained for lizardite, antigorite and chrysotile varieties are in good agreement with those presented by Rinaudo *et al.* [16]. The modes at 230, 390, 620 and 690 cm^{-1} are similar in lizardite and chrysotile, but are shifted to lower wavenumbers in the antigorite variety. In all the serpentine polymorphs, the strong peak at 230 cm^{-1} is related to O-H-O vibrations, where O is the non-bridging oxygen of a SiO_4 tetrahedron and H is the hydrogen of the outer OH group of the adjacent layer [18,19]. The peak at 530 cm^{-1}, not present in the chrysotile variety and associated to the deformation of SiO_4-AlO_4 tetrahedra, is shifted to higher wavenumbers with respect to the 510 cm^{-1} value reported in literature [16,20]. On the contrary, the peak here observed at 621 cm^{-1} corresponds to that reported at 630 cm^{-1} [21].

In the Raman spectrum of antigorite there is no evidence of the peak at 520 cm^{-1}, reported in literature and associated to deformation vibrations of the silicon oxygen layer [20]. On the other hand, the presence of a peak at 1044 cm^{-1}, due to the anti-symmetric stretching mode (ν_{as}) of Si-O_b-Si groups [20], has proven to be decisive for the discrimination of antigorite to the other polymorphs.

It has been proved that low-wavenumbers spectra of the other varieties of the serpentine group are comparable to each other. In addition, the attribution is very complex because a small variation in the chemical composition or the presence of doping elements in the lattice may cause a change in the vibrational wavenumbers and can modify the relative intensities. Moreover, polytypism and polysomatism (i.e. in antigorite) can lead to a splitting of some of the main peaks.

The vibrations of the OH groups of water molecules play a decisive role in the discrimination of the polymorph phases. OH group is a powerful probe to investigate the local geometry at the atomic scale, being very sensitive to variations in the geometry of the layers. Even cell size, symmetry and octahedral sites occupancy (cation substitutions) influence the number and position of the OH

stretching bands [8,22]. For this reason, each polymorph shows a characteristic doublet (Fig. 2), indicating the kind of local arrangement of the structure. The precise attribution of the Raman peaks in the high-wavenumbers part of the spectra, in terms of vibrations of the different OH groups occurring in the serpentine polymorphs, was obtained by Auzende *et al.* [8] investigating the behavior of serpentine minerals at increasing pressures. The vibrations of the outer hydroxyl groups are assigned to the strongly pressure-dependent modes, while the inner ones are allocated to those less pressure sensitive [8]. The new assignment of the OH stretching bands allows a better attribution of the various OH bands to the different serpentine polymorphs, with a unique correspondence. Lizardite shows two intense peaks at 3683 and 3703 cm^{-1}. Chrysotile displays the main peak at 3698 cm^{-1}, with a shoulder at 3691 cm^{-1}. Polygonal serpentine, characterized by a signal intermediate between that of chrysotile and lizardite, shows the main peak at 3697 cm^{-1} and a shoulder at 3689 cm^{-1}. These varieties also show a peak of lower intensity around 3650 cm^{-1}. Finally, antigorite shows a doublet with the main peaks located at 3665 and 3695 cm^{-1}, plus a weak peak at 3619 cm^{-1}. This evident variability in the position and shape of the peaks has allowed a good discrimination of the four phases [8,17].

Analysis of the cross-sections

The acquisition of spot analyses in complex matrices is a restriction in the study of the textural relationships between the different polymorphs of the serpentine family. This limitation has been overcome by performing two-dimensional maps, linear or rectangular, with Raman spectroscopy. The maps were performed in the OH stretching spectral range: the observation of variations of the vibrational peaks of OH groups, point by point, allowed the recognition of polymorphs in complex areas. The use of gauss-lorentzian deconvolution was useful to interpret spectra obtained in spots where different serpentine polymorphs were present (Fig. S1).

The maps were acquired on thin sections obtained on complex samples, characterized by the simultaneous presence of both lamellar and fibrous varieties. Samples consist of strongly serpentinized peridotite crossed by veins of fibrous serpentine and were chosen after a careful characterization with both optical and electronic microscopies.

We report, as an example, the investigation performed on two thin sections (Kn2, Kn3), to introduce the methodology and to show the results obtainable on serpentinite polymorphs. The complete petrographical characterization of the serpenitinites of Koniambo massif, including a more detailed interpretation of the petrological meaning of the microscopical textural relationship between the different polymorphs, is outside the scope of this work and it will be the subject of a future article.

Sample Kn2 consists of a vein of considerable size (~5 cm) of fibrous serpentine, formed by several overlapping layers (Fig. S2). Petrographic microscope observation (Fig. S3 a,b) shows the presence of several layers, not optically homogeneous, characterized by intersecting and overlying micrometric veins of the different varieties. Indeed, we can recognize that secondary veins consist of fibrous and not fibrous varieties, and none of the four varieties of the serpentine group can be excluded. Moreover, we found a considerable amount of magnetite and reddish-brown crystals of chromite (Fig. S4). Secondary electron SEM images are instead rather homogeneous, due to the trivial chemical differences between the polymorphs (Fig. S5). Microanalysis (EDS) confirms the homogeneous chemical composition. On the sample Kn2, we acquired three different Raman maps. The map of figure 3 was taken in one of the layers: from the analysis of the Raman spectra in the OH region, we have evidence a micrometric antigorite vein inside a chrysotile one, not visible by the conventional optical microscopy techniques. This suggests a first crystallization of chrysotile and then, after opening of the vein, a new crystallization of antigorite or partial re-transformation of chrysotile into antigorite. The crystallization of the higher temperature polymorph antigorite implies that this occurred in an episode of reheating: this situation, evidenced by Raman mapping, is the opposite of what one usually expects, where chrysotile is formed by transformation of antigorite at

low temperatures [23]. Conversely, the Raman map shown in figure 4, displays a more usual condition, where a micrometric chrysotile vein lies between two antigorite ones. The two maps, showing different geological process, have been experienced on different areas of the same thin-section, stressing the need of micro-mapping techniques for the understanding of the serpentinization process at microscopic scale. The last map obtained in the Kn2 sample (Fig. 5) was performed on a contact point between two veins of lizardite and antigorite: it suggests that lizardite and antigorite are not in direct contact but being separated by a fibrous chrysotile skin, not previously detected. Chrysotile could be originated by the transformation of both polymorphs, lizardite and antigorite, at low temperature.

Sample Kn3 consists of harzburgite crossed by an antigorite vein of considerable size. Both the peridotite matrix and the vein have been analyzed (Fig. S6). Petrographic microscope observation of the peridotite assemblage (Fig. S3 c,d) shows residual crystals of olivine surrounded by blades of serpentine, forming the so-called *mesh texture* [24–26]. The original appearance of the rock is preserved. Locally, the texture becomes finer and more dense: here we can observe the presence of some brownish fibers associated with whitish larger veins. By means of Raman spot analyses these brownish crystals have been identified as stichtite, an hydrated carbonate of Mg and Cr (ideal formula $Mg_6Cr_2(OH)_{16}[CO_3]\cdot 4H_2O$), which is usually formed by secondary alteration of chromium-rich serpentinite rocks. The acquisition of a map in this area (Fig. 6) evidenced the heterogeneity of the serpentine veins even at micrometric scale: an isotropic whitish vein of polygonal serpentine, easily discriminated by its Raman features in the OH stretching region, crosses a network of veins of lizardite and stichtite crystals. Minor antigorite, not visible by polarizing microscope or SEM images, is detected in the cracks.
Optical microscope images of the large antigorite vein present in the same sample (Fig. S3 e,f) show the typical non-pseudomorphic texture (*interpenetrating texture* [24,25]) of the antigorite variety. Among the antigorite lamellae, some micrometric fibrous veins of chrysotile appear. Raman mapping (Fig. 7) has shown that the contact between the fibrous chrysotile and the antigorite lamellae is not straightforward, but accretion and overlap of the two polymorphs occur.

Conclusions

The experimental method developed in this work allowed the full characterization of the serpentinization process of the studied samples. The observation of thin sections by means of optical and scanning electron microscopy permits a first evaluation of the polymorph type of serpentine and provides information about the allocation of the different varieties. The optical recognition of the possible textures (e.g. *mesh texture*, *interpenetrating texture*, *bastite*) and the study of the characteristic morphological appearance allows a first qualitative assignment of the serpentine minerals. The involvement of Raman spectroscopy in the study of the polymorphs of serpentine enabled the recognition of these minerals right on the thin sections. The identification of the varieties occurs immediately, with rapid acquisitions (few minutes) directly on the fibers (or on lamellae) embedded in their textural context. Raman peaks observed in the high-wavenumber spectral range (3550-3850 cm^{-1}), due to the stretching vibrations of the OH groups of the water molecules, have provided unique information about the attribution of the four polymorphs lizardite, antigorite, chrysotile and polygonal serpentine. The introduction of Raman micro-mapping has allowed to study the relationship between the different varieties of serpentine at a micrometric scale. This strategy has proven very effective in the study of mineralogical-petrologic samples. It can be extended to other fields of investigation such as building materials or soil decontamination, and also in the analysis of lung tissue biological-histological samples of patients suffering from asbestosis or pleural mesothelioma.

References

[1] B. W. Evans, K. Hattori, A. Baronnet, *Elements* **2013** ; *9*, 99.

[2] S. Guillot, K. Hattori, *Elements* **2013** ; *9*, 95.

[3] F. J. Wicks, D. S. O'Hanley, *Rev. Mineral. Geochemistry* **1988** ; *19*, 91.

[4] S. W. Bailey, *Rev. Mineral. Geochemistry* **1988** ; *19* , 1.

[5] E. J. W. Whittaker, J. Zussman, *Mineral. Mag. J. Mineral. Soc.* **1956** ; *XXXI*, 107.

[6] E. Burzo, *Magnetic Properties of Non-Metallic Inorganic Compounds Based on Transition Elements, Phyllosilicates*, (Ed. H. P. J. Wijn), Landolt Börnstein, Berlin, **2009** , pp. 4-21.

[7] R. H. Mitchell, A. Putnis, *Can. Mineral.* **1988** ; *26*, 991.

[8] A. L. Auzende, I. Daniel, B. Reynard, C. Lemaire, F. Guyot, *Phys. Chem. Miner.* **2004** ; *31*, 269.

[9] B. Fubini, C. Otero Arean, *Chem. Soc. Rev.* **1999** ; *28*, 373.

[10] B. Fubini, I. Fenoglio, *Elements* **2007** ; *3*, 407.

[11] S. H. Constantopoulos, *Regul. Toxicol. Pharmacol.* **2008** ; *52*, S110.

[12] H. Yang, J. R. Testa, M. Carbone, *Curr. Treat. Options Oncol.* **2008** ; *9*, 147.

[13] C. Viti, M. Mellini, *Eur. J. Mineral.* **1997** ; *9*, 585.

[14] M. Mellini, Y. Fuchs, C. Viti, C. Lemaire, J. Linarès, *Eur. J. Mineral.* **2002** ; *14*, 97.

[15] C. Groppo, C. Rinaudo, S. Cairo, D. Gastaldi, R. Compagnoni, *Eur. J. Mineral.* **2006** ; *18*, 319.

[16] C. Rinaudo, D. Gastaldi, E. Belluso, *Can. Mineral.* **2003** ; *41*, 883.

[17] C. Lemaire, F. Guyot, B. Reynard, *Eur. Union Geosci.* **1999** ; *10* , 654.

[18] W. P. Griffith, *J. Chem. Soc. A Inorganic, Phys. Theor.* **1969** ; 1372.

[19] E. Loh, *J. Phys. C Solid State Phys.* **1973** ; *6*, 1091.

[20] A. Lazarev, *Vibrational Spectra and Structure of Silicates*, Consultant Bureau, New York, **1972**.

[21] J. T. Kloprogge, R. L. Frost, L. Rintoul, *Phys. Chem. Chem. Phys.* **1999** ; *1*, 2559.

[22] E. Balan, A. M. Saitta, F. Mauri, C. Lemaire, F. Guyot, *Am. Mineral.* **2002** ; *87*, 1286.

[23] R .G. Berman, *J. Petrol.* **1988** ; *29*, 445.

[24] F. J. Wicks, E. J. W. Whittaker, *Can. Mineral.* **1977** ; *15*, 459.

[25] D. O'Hanley, *Serpentinites: Records of tectonic and petrological history*, Oxford University Press, London, **1996**.

[26] C. Viti, M. Mellini, *Eur. J. Mineral.* **1998** ; *10*, 1341.

Figure and Table captions

Figure 1 Raman spectra obtained at 632.8 nm in the low-wavenumbers region of chrysotile, antigorite and lizardite.

Figure 2 Raman spectra obtained at 473.1 nm in the high-wavenumbers region of polygonal serpentine, chrysotile, antigorite and lizardite.

Figure 3 Raman map on the sample Kn2 obtained in the OH stretching region. Green: chrysotile; red: antigorite.

Figure 4 Raman map on the sample Kn2 obtained in the OH stretching region. Green: chrysotile; red: antigorite.

Figure 5 Raman map on the sample Kn2 obtained in the OH stretching region. Green: chrysotile; red: antigorite; blue: lizardite.

Figure 6 Raman map on the sample Kn3 obtained in the OH stretching region. Yellow: polygonal serpentine; green: chrysotile; red: antigorite; blue: lizardite.

Figure 7 Raman map on the sample Kn3 obtained in the OH stretching region. Green: chrysotile; red: antigorite.

Figure S1 Example of Raman spectrum showing the simultaneous presence of the main peaks of chrysotile, antigorite and lizardite minerals (473.1 nm, high-wavenumbers region). In this rare case it is hard to distinguish the polygonal serpentine from chrysotile variety.

Figure S2 Outcrop showing the vein of fibrous serpentine where sample Kn2 is taken.

Figure S3 Polarizing microscope images with parallel (left column) and crossed (right column) polarizers of the thin sections obtained from samples Kn2 (a,b), Kn3-peridotitic matrix (c,d) and Kn3-antigorite vein (e,f).

Figure S4 Raman spectra obtained at 632.8 nm in the low-wavenumbers region of chromite (top) and magnetite (bottom). * = calibration lamp.

Figure S5 Secondary electron SEM image of sample Kn2. Only chromite crystal is evidenced, the veins structure is not clearly visible.

Figure S6 Harzburgite outcrop crossed by an antigorite vein, where sample Kn3 was taken.

Table 1 Assignment of peaks in the Raman spectra at low- and high-wavenumbers regions of the main serpentine phases studied in this work and compared with results obtained by Groppo *et al.* (2006) and Auzende *et al.* (2004).

Lizardite			Antigorite			Chrysotile			Polygonal serpentine		Attribution
This work	Groppo *et al.* (2006)	Auzende *et al.* (2004)	This work	Groppo *et al.* (2006)	Auzende *et al.* (2004)	This work	Groppo *et al.* (2006)	Auzende *et al.* (2004)	This work	Auzende *et al.* (2004)	
230 s	233	241	229 vs	230	235	232 vs	231	235		236	Vibrations O-H-O *
349 w	350	351	-	-	-	345 w	345	346		647	δ SiO_4
386 vs	388	393	377 vs	375	377	388 vs	389	391		391	Symmetric ν_5 SiO_4 **
532 m	510	527	-	520	528	-	-	-		-	Deformation SiO_4-AlO_4 ***
621 m	630	-	631 m	635	-	622 w	620	-		-	Translation OH-Mg-OH *
689 s	690	695	687 s	683	685	691 vs	692	694		696	ν_s Si-O_b-Si
-	-	-	1045 m	1044	-	-	-	-		-	ν_{as} Si-O_b-Si ***
-	1096 ?	-	-	-	-	-	1105	-		-	ν_{as} Si-O_{nb}
3660 w		3654	-		3641	3651 w		3649	3646 w	3646	ν_s outer OH ****
3683 vs		3688	3665 vs		3666	3691 sh		3691	3689 sh	3689	ν_s outer OH ****
3703 vs		3704	3695 vs		3693	3698 vs		3699	3697 vs	3697	ν_s inner OH ****

vs very strong, s strong, m medium, w weak, vw very weak, sh shoulder. The band wavenumber is reported in cm^{-1}.
* [16]. ** [21]. *** [20], **** [8].

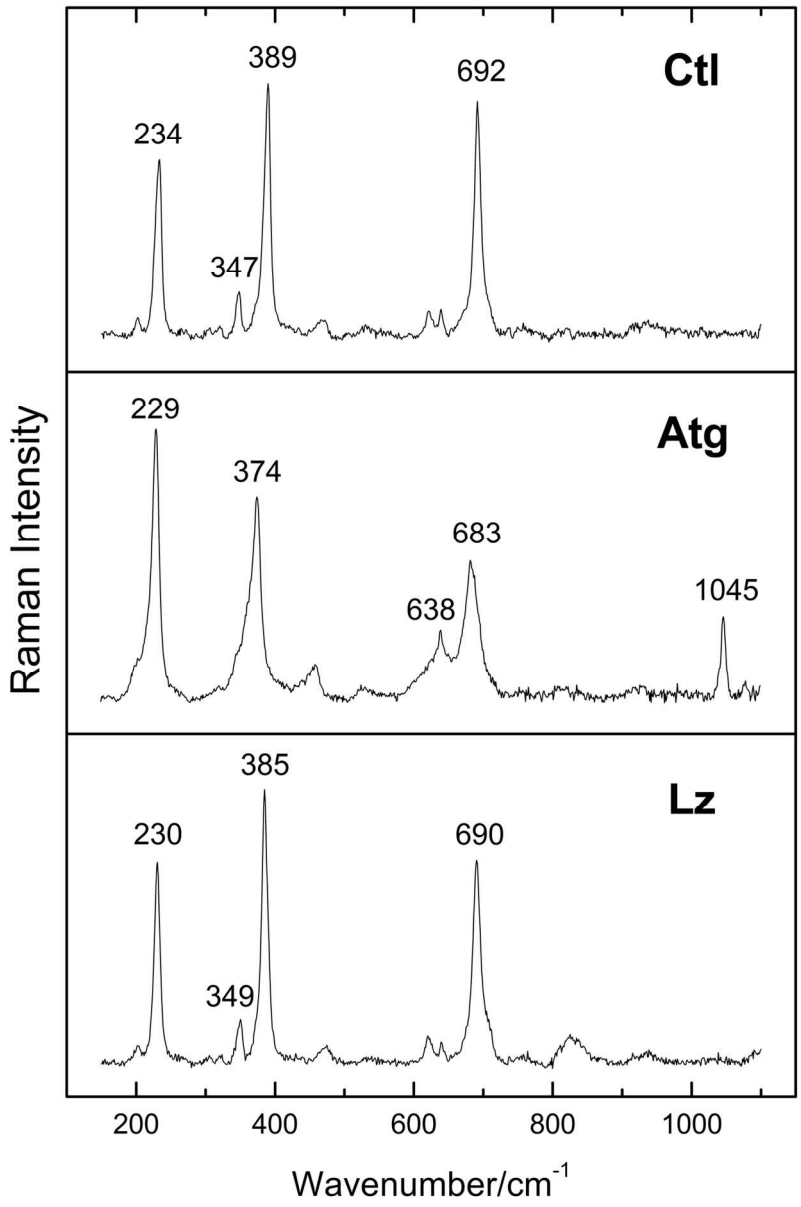

Figure 1 Raman spectra obtained at 632.8 nm in the low-wavenumbers region of chrysotile, antigorite and lizardite.
120x180mm (300 x 300 DPI)

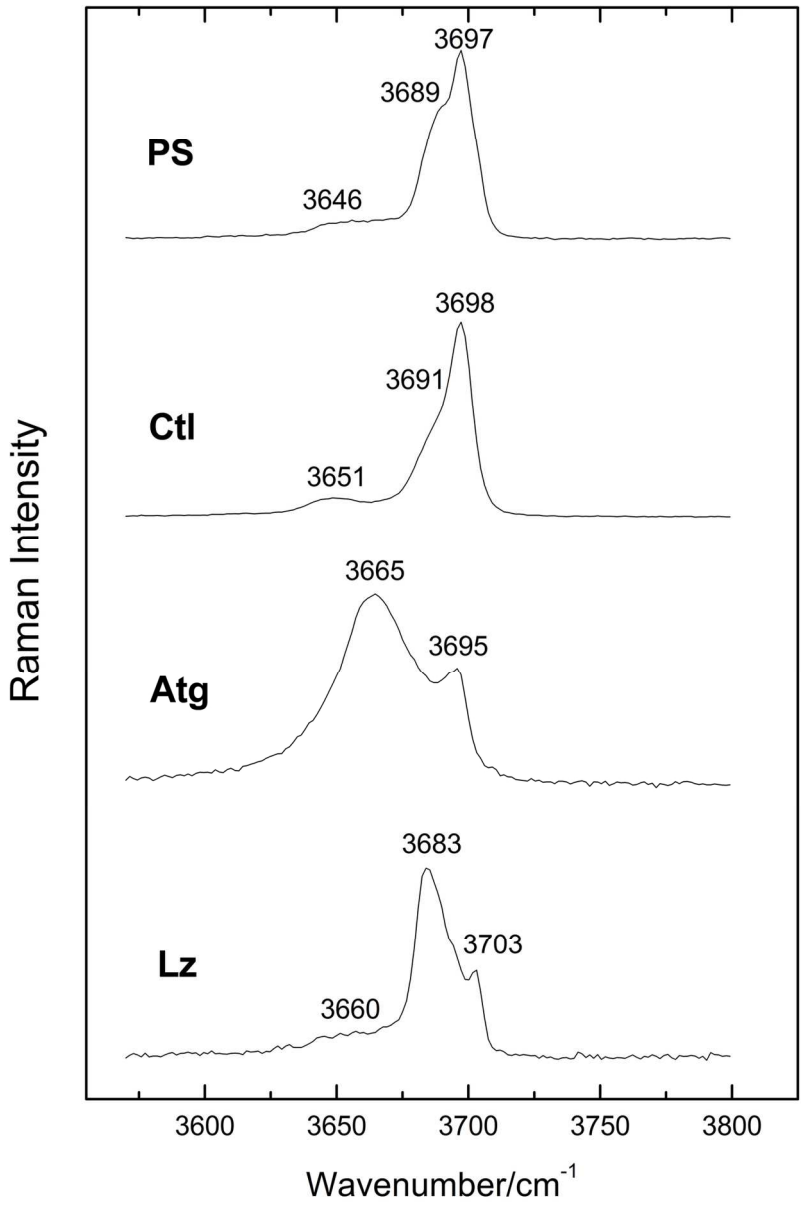

Figure 2 Raman spectra obtained at 473.1 nm in the high-wavenumbers region of polygonal serpentine, chrysotile, antigorite and lizardite.
119x179mm (300 x 300 DPI)

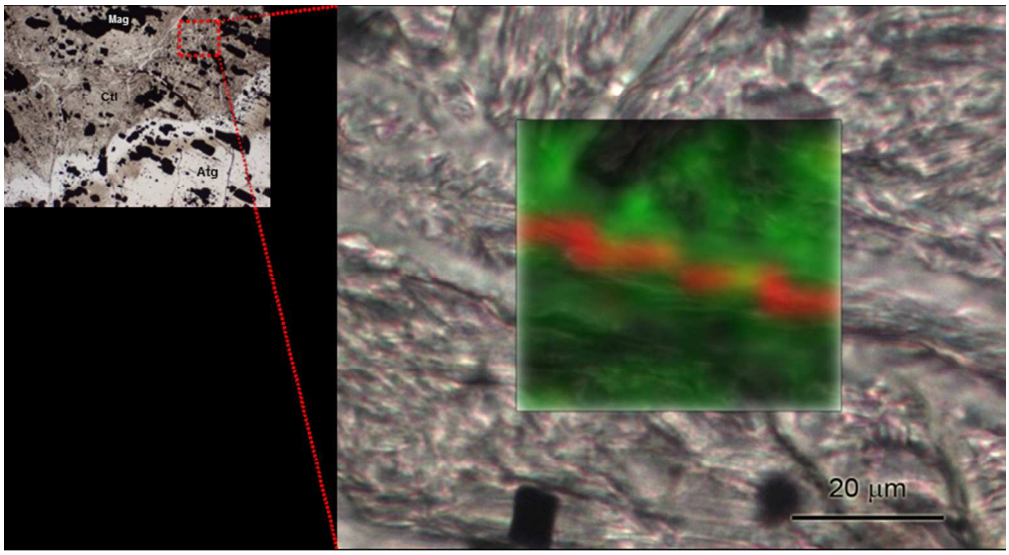

Figure 3 Raman map on the sample Kn2 obtained in the OH stretching region. Green: chrysotile; red: antigorite.
150x81mm (150 x 150 DPI)

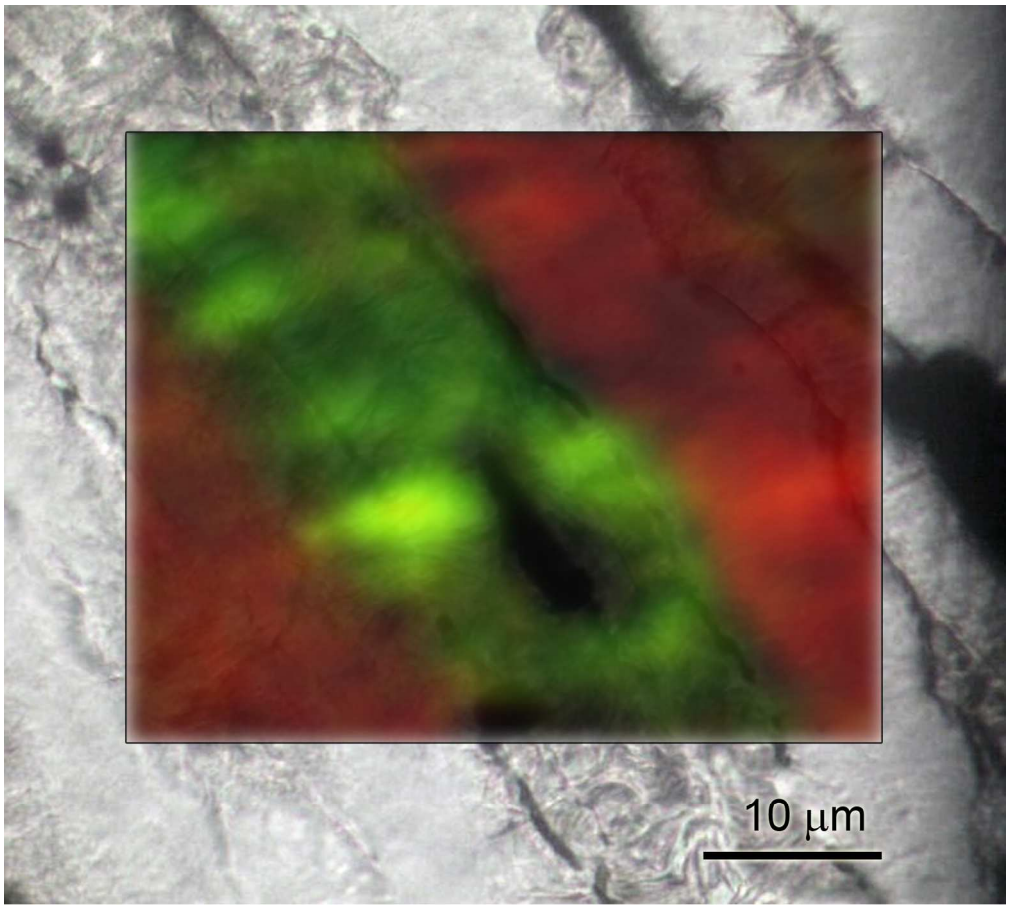

Figure 4 Raman map on the sample Kn2 obtained in the OH stretching region. Green: chrysotile; red: antigorite.
705x634mm (72 x 72 DPI)

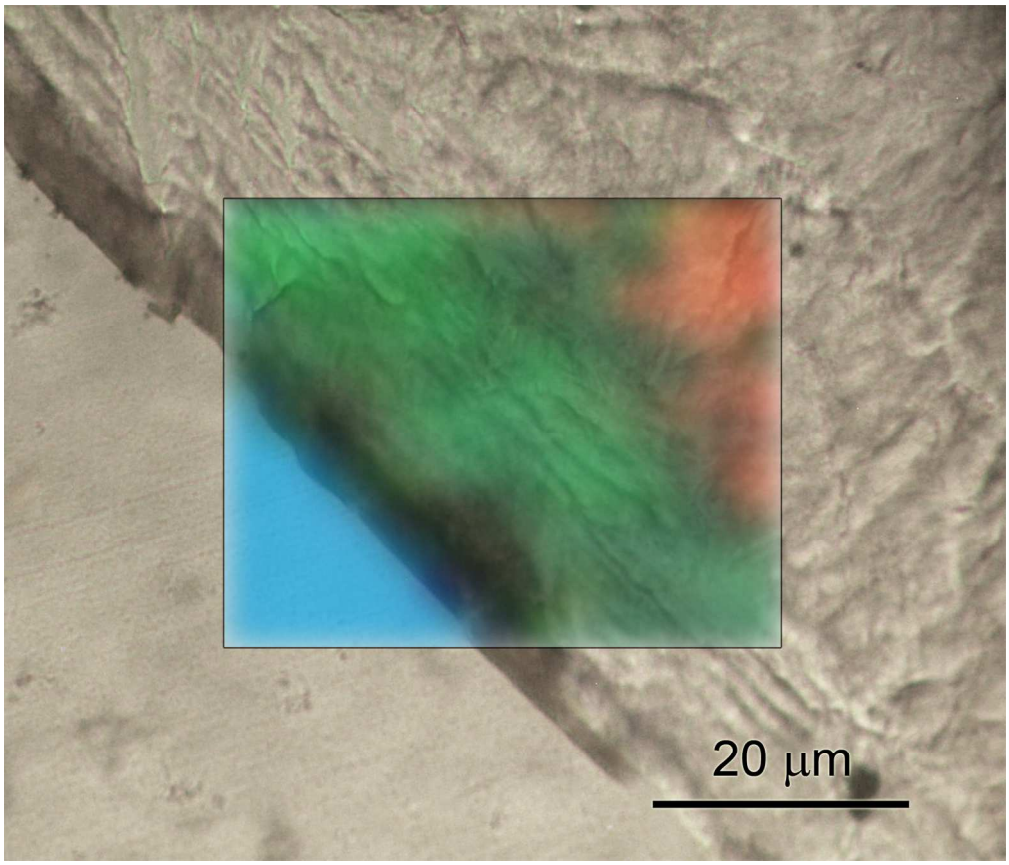

Figure 5 Raman map on the sample Kn2 obtained in the OH stretching region. Green: chrysotile; red: antigorite.
705x602mm (72 x 72 DPI)

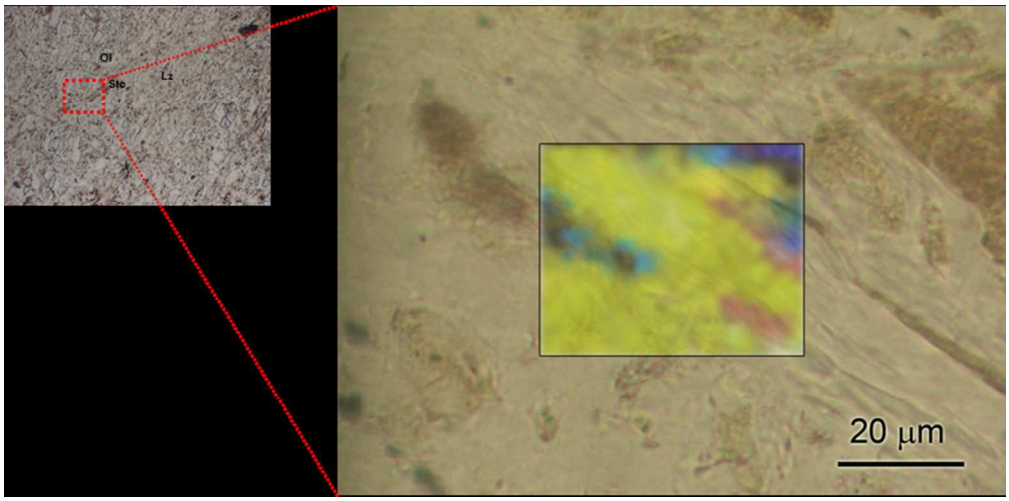

Figure 6 Raman map on the sample Kn3 obtained in the OH stretching region. Yellow: polygonal serpentine; green: chrysotile; red: antigorite; blue: lizardite.
149x73mm (150 x 150 DPI)

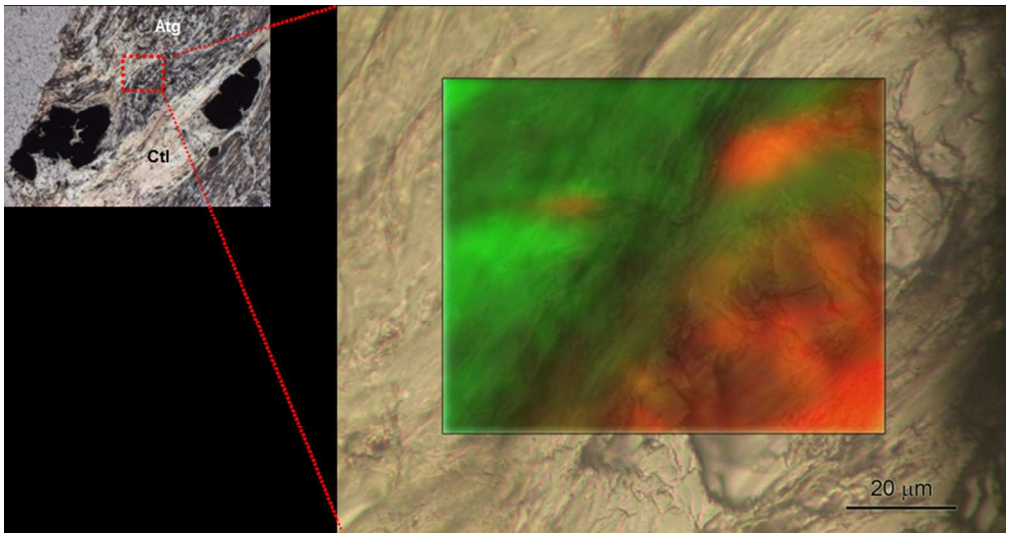

Figure 7 Raman map on the sample Kn3 obtained in the OH stretching region. Green: chrysotile; red: antigorite.
150x79mm (150 x 150 DPI)